Logical devices implemented using quantum cellular automata

P. Douglas Tougaw and Craig S. Lent
Department of Electrical Engineering, University of Notre Dame, Notre Dame, Indiana 46556

(Received 28 July 1993; accepted for publication 26 October 1993)

We examine the possible implementation of logic devices using coupled quantum dot cells. Each quantum cell contains two electrons which interact Coulombically with neighboring cells. The charge distribution in each cell tends to align along one of two perpendicular axes, which allows the encoding of binary information using the state of the cell. The state of each cell is affected in a very nonlinear way by the states of its neighbors. A line of these cells can be used to transmit binary information. We use these cells to design inverters, programmable logic gates, dedicated AND and OR gates, and non-interfering wire crossings. Complex arrays are simulated which implement the exclusive-OR function and a single-bit full adder.

I. INTRODUCTION

Devices based on quantum-mechanical principles hold the promise of faster speeds and greatly reduced sizes. Most quantum device designs examined have been similar to classical device implementations in that they use currents and voltages to encode information. Thus although the device operations proposed have been based on quantum physics, the architectures have been conventional.

Employing quantum structures in conventional architectures has proven problematic for reasons directly related to the inherently small size of quantum-effect devices. The output signal of such ultrasmall devices, which is typically nanoamperes of current, must be able to drive several other similar devices, which may require a change of many millivolts in their input voltages. Another significant problem is that the capacitance of interconnecting wires tends to dominate the device behavior.[1] The wiring problem is aggravated by the fact that energy must be supplied to each computational element through power connections.

We have recently proposed a scheme in which Coulomb-coupled quantum devices are connected in a cellular automata architecture.[2] We call such architectures quantum cellular automata (QCA).[3–6] A QCA consists of an array of quantum-dot cells connected locally by the interactions of the electrons contained in each cell. The scheme is non-conventional in that the quantum state of each cell is used to encode binary information. The Coulomb interaction connects the state of one cell to the state of its neighbors. Thus the problems associated with small output currents and parasitic capacitances of connecting wires do not occur. "Binary wires" composed of linear arrays of cells are effective in transmitting information, coded in the cell states, from one place to another.[5]

In this paper we present simulations of QCA arrays, some of which are quite large, performing complex computational tasks. We review the basic cell operation and the use of linear arrays as a binary wire. Novel programmable logical gates and inverters are simulated and provide the basis for computing in this scheme. We demonstrate that it is possible to cross two QCA binary wires in the plane, with no interference. Building up more complicated operations from the basic gates, we simulate QCA implementations of an exclusive-OR function and a full adder. This serves to demonstrate that the interactions between cells are sufficiently local that hierarchical design is possible.

The calculations presented here are for zero temperature and assume the several-electron system has relaxed to its ground state before a valid output is read. Unlike conventional digital devices, the QCA operates on the principle that inelastic processes will always tend to drive the system back to its ground state.[7] The time evolution of the many-electron state of the system will in general be very complicated, but only the final ground-state properties are used for computing. Applying a new set of inputs places the system in an excited state. While the system is relaxing (presumably through a complicated process of exchanging energy with its environment), the outputs are not valid. Once the system has settled into its new ground state, the results of the calculation appear encoded in the states of the output cells located at an edge of the array. This idea of "computing with the ground state" is discussed at length in Ref. 4.

In the next section, we will give a review of QCA theory and the operation of the "standard cell." The standard cell is the most thoroughly studied cell design because it combines physically reasonable design parameters with excellent bistable saturation. A detailed treatment of the cell, various related cell designs, and our self-consistent calculations for arrays of coupled cells can be found in Refs. 3–6. Section II D discussed how lines of cells can be used to transmit information using a QCA binary wire. Section III shows a design for an inverter, and Sec. IV deals with the influence of several neighboring cells on the cell states. This leads to the idea of the majority voting logic gate and we demonstrate how its behavior can be used to implement a programmable AND/OR gate. Section V demonstrates a noninterfering planar crossing of two QCA wires. Section VI shows how these various ideas can be combined to form an exclusive-OR and a full adder.

II. COUPLED QUANTUM CELLS

The standard cell design, shown schematically in Fig. 1(a), consists of five quantum dots located at the corners and the center of a square. The cell is occupied by a total

 0021-8979/94/75(3)/1818/8/$6.00

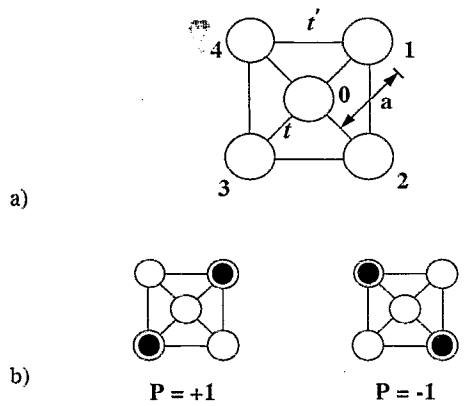

FIG. 1. Schematic of the basic five-site cell. (a) The geometry of the cell. The tunneling energy between the middle site and an outer site is designated by t, while t' is the tunneling energy between two outer sites. (b) Coulombic repulsion causes the electrons to occupy antipodal sites within the cell. These two bistable states result in cell polarizations of $P=+1$ and $P=-1$ [see Eq. (1)].

of two electrons hopping among the five sites. Tunneling occurs between the central site and all four of the outer sites (near-neighbor tunneling) and to a lesser degree between neighboring outer sites (next-near-neighbor tunneling). It is assumed that the potential barriers *between* cells are high enough to completely suppress intercellular tunneling.

The electrons tend to occupy antipodal outer sites within the cell due to their mutual electrostatic repulsion as shown in Fig. 1(b). The two stable states shown are degenerate in an isolated cell, but an electrostatic perturbation in the cell's environment (such as that caused by neighboring cells) splits the degeneracy and causes one of these configurations to become the cell ground state. Altering the perturbation causes the cell to switch between the two states in an abrupt and nonlinear manner. This very desirable bistable saturation behavior is due to a combination of quantum confinement, Coulombic repulsion, and the discreteness of electronic charge.

A. Cell polarization

Since Coulomb repulsion causes the electrons to occupy antipodal sites, the ground state charge distribution may have the electrons aligned along either of the two diagonal axes shown in Fig. 1(b). We therefore define the cell polarization, a quantity which measures the extent to which the charge distribution is aligned along one of these axes. The polarization is defined as

$$P \equiv \frac{(\rho_1+\rho_3)-(\rho_2+\rho_4)}{\rho_0+\rho_1+\rho_2+\rho_3+\rho_4}, \tag{1}$$

where ρ_i denotes the electronic charge at site i. As shown in Fig. 1(b), electrons completely localized on sites 1 and 3 will result in $P=1$, while electrons on sites 2 and 4 yield $P=-1$. An isolated cell would have a ground state which is an equal combination of these two states and would therefore have a net polarization of zero.[8]

B. Standard cell parameters

We employ a simple model of the standard quantum cell, representing the quantum dots as sites and ignoring any degrees of freedom internal to the dot. We use a second-quantized Hubbard-type Hamiltonian in the basis of two-particle site kets for this model. The Hamiltonian includes terms for the on-site energy (the cost to confine a single electron to a site), tunneling between all pairs of the five sites, Coulombic interaction between the charge densities on each pair of sites, and the on-site charging energy of each site (the purely Coulombic cost for two electrons of opposite spin to occupy the same dot). The Hamiltonian for a single isolated cell can be written as

$$H_0^{\text{cell}} = \sum_{i,\sigma} E_0 n_{i,\sigma} + \sum_{i>j,\sigma} t_{i,j}(a_{i,\sigma}^{\dagger} a_{j,\sigma} + a_{j,\sigma}^{\dagger} a_{i,\sigma}) + \sum_i E_Q n_{i,\uparrow} n_{i,\downarrow} + \sum_{i>j,\sigma,\sigma'} V_Q \frac{n_{i,\sigma} n_{j,\sigma'}}{|\mathbf{R}_i - \mathbf{R}_j|}. \tag{2}$$

Here $a_{i,\sigma}$ is the second-quantized annihilation operator which destroys a particle at site i ($i=0,1,2,3,4$) with spin σ, and $a^{\dagger}_{i,\sigma}$ is the creation operator for a similar particle. The number operator for site i and spin σ is represented by $n_{i,\sigma}$. The values of the physical parameters used are based on a simple, experimentally reasonable model. We take E_0 (the on-site energy) to be the ground state energy of a circular quantum dot of diameter 10 nm holding an electron with effective mass $m^*=0.067\ m_0$. The near-neighbor distance between dot centers a is taken to be 20 nm. The Coulomb coupling strength V_Q is calculated for a material with a dielectric constant of 10, and E_Q, the on-site charging cost, is taken to be $V_Q/(D/3)$.[9] The tunneling energy between an outer dot and the central dot is $t=0.3$ meV, and the next-near neighbor coupling connecting the outer dots, t', is taken to be $t/10$.[10] To maintain charge neutrality in the cell, a fixed positive charge $\tilde{\rho}=(2/5)e$ is placed on each site.[11]

The spins of the two electrons in the cell can be either parallel (the triplet spin state) or antiparallel (the singlet spin state). We consider here the case of electrons with antiparallel spins, since that is the ground state of the cell. Calculations with electrons having parallel spins yield qualitatively very similar results.

The interaction of a nonisolated cell with its electrostatic environment (including neighboring cells) is included by altering the on-site energies to account for the potential due to charge on each site of all the neighboring cells. We then solve the time-independent Schrödinger equation in the basis of two-particle site kets to find the eigenstates of the system. The charge on each site can be calculated by finding the expectation value of the number operator in the ground state $\rho_i=-e\langle\hat{n}_i\rangle$. These site charges can be used to calculate the cell polarization P using Eq. (1).

For a system composed of many cells, the ground state of the entire system is found by iteratively solving for the ground state of each cell. We treat the physics within the cell as before, including exchange and correlation effects exactly. The intercellular interaction is treated self-

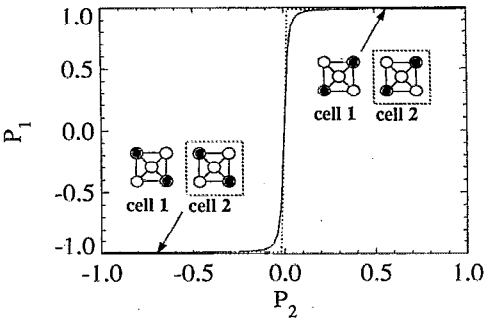

FIG. 2. Cell–cell response function for the basic five-site cells shown in the insets. This shows the polarization P_1 induced in cell 1 by the fixed polarization of its neighbor P_2. The solid line corresponds to the triplet state, and the dotted line to the singlet state. The two are nearly degenerate except for very small values of P_2.

consistently using a Hartree approximation. This method, called the intercellular Hartree approximation (ICHA) is discussed in Refs. 4 and 5.

C. Calculating the cell–cell response function

To be useful in cellular automata-type architectures, the state of a cell must be strongly influenced by the states of neighboring cells. To demonstrate how one of these model cells is influenced by the state of its neighbor, consider the two cells shown in the insets to Fig. 2. These are two of the standard cells described above, and their centers are separated by a distance of $3a=60$ nm. We assume cell 2 has a given polarization P_2 and that the electron probability density on the central site is negligible. This means that the charge distribution is completely determined by the cell polarization. We calculate the electrostatic potential at each site of cell 1. This additional environmental potential energy is then included in the Hamiltonian of cell 1. The two-electron time-independent Schrödinger equation is solved for a series of values of P_2 in the range $[-1,+1]$. The ground state polarization of cell 1, P_1, is then computed for each value of P_2. Thus, we can plot the *induced* polarization of cell 1 as a function of the polarization of cell 2. This function, $P_1(P_2)$, which we call the cell–cell response function, is one measure of how well a cell will operate in a quantum cellular automata architecture.

Figure 2 shows the cell–cell response function for the standard cell. The highly nonlinear nature of the response indicates that a small polarization in cell 2 causes a very strong polarization in its neighbor, cell 1. Figure 2 also shows that the polarization of cell 1 *saturates* very quickly to a value of $+1$ or -1. This bistable saturation is the basis of the quantum cellular automata since it means that one can encode bit information using the cell polarization. We assign the bit value of 1 to the $P=+1$ state and the bit value 0 to the $P=-1$ state. Since the cell is almost always in a highly polarized state ($|P|\cong 1$), the state of the cell will be indeterminate only if the electrostatic environment due to other cells is perfectly symmetric. Reference 6 examines the cell–cell response for various cell designs.

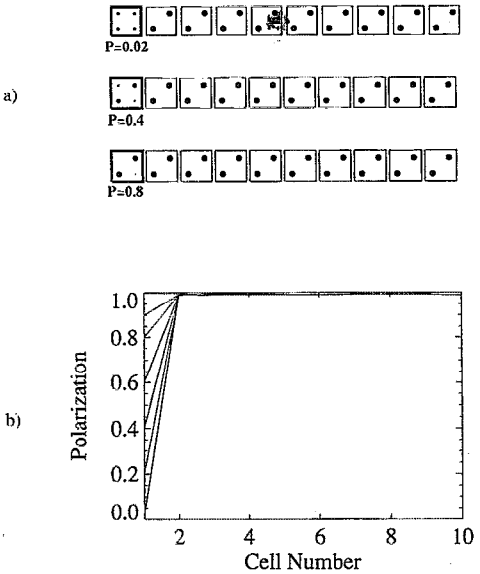

FIG. 3. A QCA wire. (a) Three binary wires being driven from the left. In each case, a weakly polarized driver induces full polarization in the rest of the wire. This allows the transmission of information down the length of the wire. The diagram is not simply schematic. The diameter of each dot shown is proportional to the charge on the corresponding site, obtained from a self-consistent solution for the ground state charge distribution in this system. (b) Polarization of the wire cells for various values of the driver cell polarization. The wires rapidly recover from a weak driver and maintain full polarization through their entire length.

D. The binary wire

Since the polarization of each cell tends to align with that of its neighbors, a linear arrangement of standard cells can be used to transmit binary information from one point to another. Figure 3(a) shows three such lines of cells in which the polarization of the left-most cell is fixed and the other cells are free. In each case, all of the free cells align in the same direction as the driving cell, so the information contained in the state of the driver is transmitted down the wire.

The three different systems in Fig. 3(a) each show a different polarization of the driving cell. In each case the free cells are nearly completely polarized. Figure 3(b) shows plots of the polarization of a line of cells for various values of polarization in the driver cell. As in Fig. 3(a), we see that the polarizations of the free cells rapidly recover from a weakly polarized driver and maintain full polarization throughout the line. The wire is robust in the sense that it transmits a binary value (corresponding to a polarization of roughly $+1$ or -1) even if the driver, or any intermediate cells, are weakly polarized. The nonlinear response of the cell to the polarization of its neighbors plays the role of gain in a conventional digital circuit. It restores the signal to the "signal rails." The wire is also therefore robust against cell-to-cell variations in the cell parameters. Precise control of cellular geometry or tunneling rates is not required. Further discussion of such lines of cells can be found in Ref. 5.

It is important to note that unless stated otherwise, these figures are not simply schematic, but plots of the

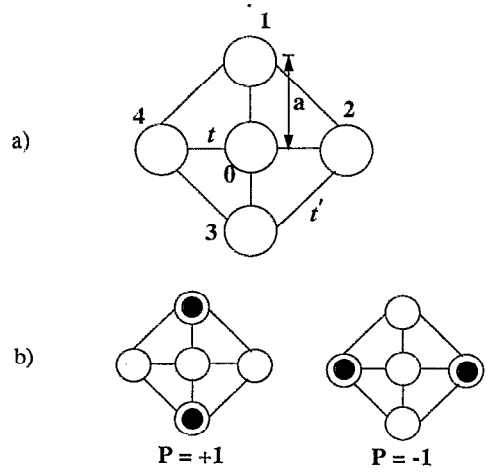

FIG. 4. A "rotated" QCA cell. (a) The rotated cell is identical in all ways to the standard cell except it is rotated by 45°. This causes the dots within the cell to have a vertical and horizontal placement relative to each other. (b) The polarizations of neighboring rotated cells tend to align opposite each other as shown here schematically.

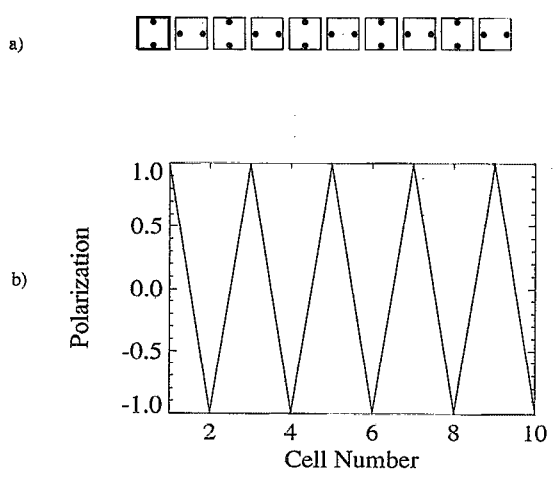

FIG. 5. An inverter chain. (a) A self-consistent solution of the ground state of a line of rotated cells. The polarization alternates direction between each pair of cells, but each cell is nearly fully polarized. (b) A polarization plot for the same system verifies nearly full polarization of every cell.

self-consistently calculated electron charge on each site. The radius of each dot is proportional to the charge at that site.

While a line of standard cells can be used to transmit information from one point to another, it is not the only way to carry out such transmission. Figure 4(a) shows a schematic diagram of a standard cell which has been rotated by 45°. In all other ways, this "rotated" cell is identical to a standard cell. Figure 4(b) shows a schematic representation of two of these rotated cells. This figure shows that the polarizations of two such neighboring cells tend to align *opposite* each other. This anti-alignment is in contrast to the behavior of standard cells in which near neighbors tend to align with each other.

Figure 5(a) shows a line of such rotated cells. The polarizations alternate along the length of the line. For this reason, we refer to a line of rotated cells as an "inverter chain." If the length of the wire is known, it is simple to determine the signal that is being sent. Thus, an inverter chain is another way quantum cells can be used to transmit information down a wire. Figure 5(b) shows a polarization plot corresponding to the inverter chain in Fig. 5(a). This figure shows that, although the polarization alternates direction between each pair of cells, its magnitude remains constant. Inverter chains like this prove useful in more complicated QCA designs.

III. A QCA INVERTER

Two standard cells in a diagonal orientation are geometrically similar to two rotated cells in a horizontal orientation. For this reason, standard cells in a diagonal orientation tend to align in opposite polarization directions as in the inverter chain. This antialigning behavior can be used in designing a QCA inverter.

Figure 6 shows an arrangement of cells that acts as an inverter. The "signal" comes in from the left on a binary wire and splits into two parallel wires which are offset from the original. Because the incoming wire extends one cell beyond the beginning of the offset wires, aligning effects dominate at the branch point. Since the horizontal and vertical interactions are dominant, the signal in the two offset wires always matches that of the incoming wire. At the right end of the inverter, the offset wires rejoin into one. However, there are no horizontal or vertical interactions at this end, so the diagonal (antialigning) interactions cause the signal to be inverted. Although Fig. 6 only shows a 1 being inverted to a 0, the design will invert a 0 also. The design shown has the added advantage that the outgoing wire is not offset from the incoming wire.

IV. PROGRAMMABLE LOGIC GATES

Figure 7(a) shows an arrangement of five standard cells. The states of the cells on the top, left, and bottom are fixed, while the center and right cells are free to react to the fixed charge. In an actual implementation, the three neighbors would not be fixed; they would be driven by results of previous calculations or by inputs at the edge of the QCA.

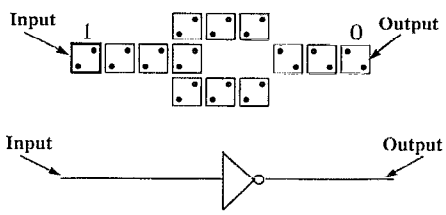

FIG. 6. A QCA inverter. The signal comes in from the left, splits into two parallel wires, and is inverted at the point of convergence. The design is geometrically symmetric, so inversion of a 1 or a 0 occurs with the same reliability. The diagram is not simply schematic. The diameter of each dot shown is proportional to the charge on the corresponding site, obtained from self-consistent solution for the ground state charge distribution. Also shown is the logic symbol for the inverter.

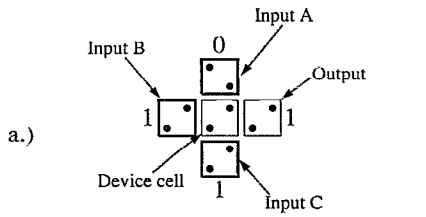

a.)

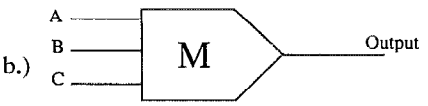

b.)

c.)

A	B	C	Out
0	0	0	0
0	0	1	0
0	1	0	0
0	1	1	1
1	0	0	0
1	0	1	1
1	1	0	1
1	1	1	1

FIG. 7. Majority voting logic. (a) The states of the center and right cells are always the same as the state of the majority of the three fixed neighbors. The cells with heavy borders have fixed charge distributions. The figure represents the self-consistent solution of the ground-state charge on each site. (b) The schematic symbol for the majority voting logic element. (c) The truth table of the majority voting logic element.

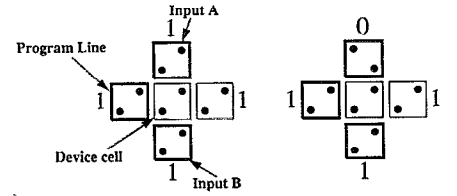

a.)

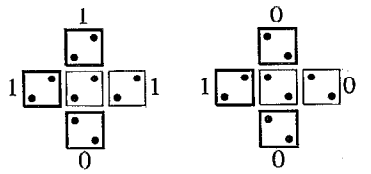

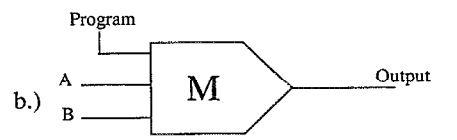

b.)

FIG. 8. The programmable AND/OR gate. (a) The program line is set to one in each system, so the gate is displaying OR logic. All four combinations of the nonprogram line inputs are shown. The cells with heavy borders have fixed charge distributions. Any one of the three inputs could be the program line; the left cell is not special. The diameter of each dot shown is proportional to the charge on the corresponding site, obtained from a self-consistent solution for the ground state charge distribution. (b) The schematic symbol for the programmable AND/OR gate.

In the particular case shown, two of the inputs are in the "one" state, and the other is in the "zero" state. When we solve for the ground state of the free cells, we find that they both match the state of the majority of the fixed neighbors. We refer to this result, which is true for all combinations of the three inputs, as *majority voting logic.*

To represent this new logical function, we will use the symbol shown in Fig. 7(b). As this symbol demonstrates, there are three inputs and one output for such a logic gate. Figure 7(c) shows the truth table for a majority voting logic gate. This is a summary of our simulation of all eight combinations of the three inputs. The majority voting logic function can be expressed in terms of fundamental Boolean operators as

$$M(A,B,C)=AB+BC+AC.$$

While it may appear that it requires five cells to implement this majority voting gate, only the center cell is actually "performing the calculation." All the other cells are part of the binary wires leading to and away from this gate. For this reason, we refer to the center cell as the "device cell."

While majority voting logic is a valuable result by itself, it is especially useful when we interpret the three inputs in a particular way. In Fig. 8(a), we have singled out one of the three inputs and called it the "program line." Because of the symmetry of the system, any of the three could serve as the program line. The one case shown (with the program line coming in from the left) is sufficient for illustration purposes. The four systems shown in Fig. 8(a) include all combinations of signals on the two nonprogram lines. Since the program line is in the one state in all four systems, it takes a zero vote from each of the other two lines to put the majority voting cell in the zero state. Thus, the system performs the OR operation on the two nonprogram lines. Likewise, if the program signal is zero, the result is also zero unless both of the other inputs are one. Such a system implements the AND operation.

By interpreting one of the inputs as a program line, we have implemented a programmable AND/OR gate. The nature of the logic performed by this gate (AND vs OR) is determined by the state of the program line, and the other two inputs are applied to the gate thus defined. As shown in Fig. 8(b), the difference between a majority voting gate and a programmable AND/OR gate is just a relabeling of one of the three inputs. The nature of the gate and the truth table it represents are identical, so we use the same device symbol to represent it.

Since the cell on the right always matches the center cell, the result of this calculation can be propagated away from the gate down a QCA wire, where it will eventually serve as an input to subsequent gates. It may at first seem that the state of the cell on the right should be counted in the majority voting logic, but this is not the case. Since it is completely free to react to the cells around it, we say that it is a "driven" neighbor for this gate. By contrast, the other three neighbors are not free to change because they are fixed by previous results or inputs directly from the edge of the QCA (we here assume that the input is fixed at the left edge of the array). We call these "driving" neighbors for this calculation. Of course, once the result of this calculation propagates away to the right, it can serve as a driving neighbor for subsequent gates.

A nonprogrammable implementation of an AND gate is shown in Fig. 9(a). In this case, the signal on the program line (which again is on the left for illustration pur-

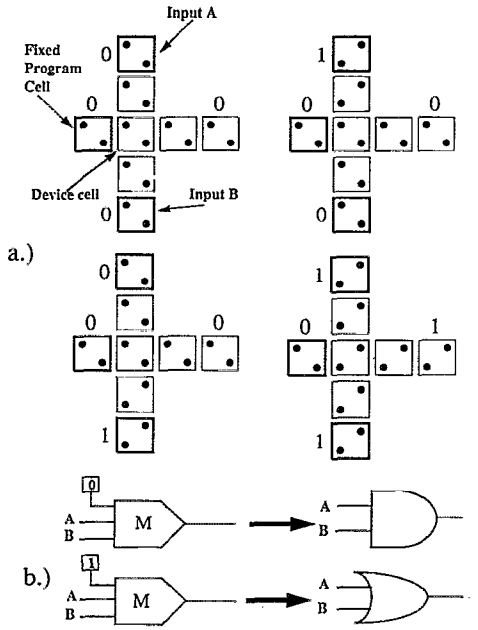

FIG. 9. (a) The dedicated AND gate. A programmable AND/OR gate can be reduced to implement a dedicated AND gate by permanently setting the program cell to 0. Likewise, a dedicated OR gate could be implemented by permanently setting it to 1. (b) A schematic diagram of how programmable gates can be "reduced" by permanently fixing the program line.

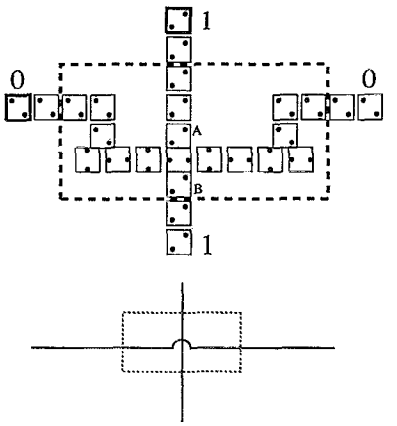

FIG. 10. A coplanar crossing of two QCA wires. The diameter of each dot shown is proportional to the charge on the corresponding site, obtained from a self-consistent solution for the ground state charge distribution. A schematic representation of a noninterfering wire crossing is also shown.

poses) is permanently fixed in the zero state. This would be done by destroying sites 1 and 3 once the cell had been fabricated. Since the gate is no longer programmable, we lose some of the flexibility originally present, but there are many situations that require such a dedicated logic element. We say that the gate has been reduced since it can now perform only one of the two functions of a programmable gate. A dedicated OR gate can be implemented in a similar way by destroying sites 2 and 4 of the program cell. Figure 9(b) shows schematically how a programmable logic gate can be converted to a dedicated two-input gate by permanently setting the value of the program line.

V. COPLANAR WIRE CROSSING

In a traditional integrated circuit, the crossing of two wires is achieved by physically passing one wire over the other with an insulator placed between them. Such a nonplanar crossing would also work for two QCA wires, but the cellular nature of such wires allows us to cross them using an entirely coplanar arrangement of cells. Such a coplanar crossing is impossible in conventional circuits which code information using currents and voltages.

Figure 10 shows one way to cross two binary wires composed of QCA cells. In this example, the horizontal line is transmitting a zero and the vertical line is transmitting a one. In order to cross the lines, the horizontal wire must be converted from standard cells to rotated cells. These rotated cells are identical to those composing the inverter chain shown in Sec. IV. The signal on the horizontal line is transmitted to the rotated cells by a special arrangement of three cells, an "$\times$-to-$+$ converter." Since the state of a normal (or "$\times$-shaped") cell has no switching effect on a rotated (or "$+$-shaped") cell directly in line with it, such conversion requires that the standard cell be above and on a line directly between two of the rotated cells. Such placement has the desired transmission effect, and a similar arrangement can also serve to convert the signal back to standard cells (a "$+$-to-$\times$ converter"). As shown in Sec. IV, the polarization of the cells in the inverter chain alternate direction beginning immediately after the $\times$-to-$+$ converter. There must therefore be an even number of cells between the $\times$-to-$+$ converter and the $+$-to-$\times$ converter.

The reason for going through this conversion to and from rotated cells has already been mentioned: the state of a normal cell has no switching effect on a rotated cell directly in line with it. Similarly, the state of a rotated cell has no effect on the state of a normal cell in line with it. We can therefore directly cross the horizontal inverter chain of temporarily rotated cells and the vertical line of normal cells without interference. This crossing relies on the coupling between cells labeled "A" and "B" in the figure. This coupling is somewhat weaker than the usual coupling between cells in a wire chain because these cells are further apart. We have verified by direct calculation of the many-electron ground state that the system correctly transmits all possible combinations of the two signals without interference.

VI. XOR AND FULL ADDER

Figure 11(a) shows a schematic of an exclusive-OR function implemented using dedicated AND and OR gates. Figure 11(b) shows one implementation of this schematic using reduced gates (acting as two AND gates and one OR gate). The noninterfering wire crossing is employed in connecting the individual gates together. Figure 11 shows the ground-state charge on each site of each cell in the array for one set of inputs. We have verified by directly calculat-

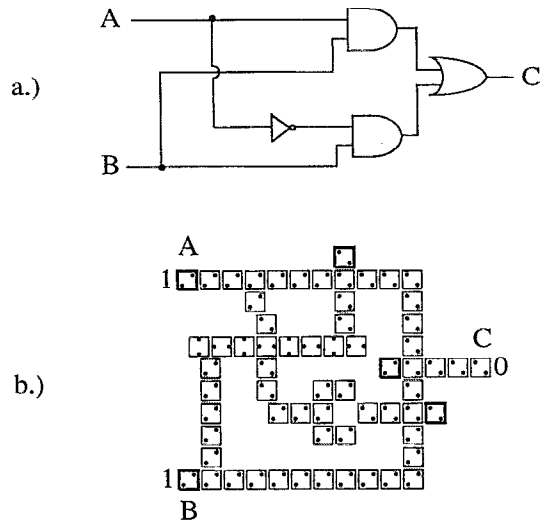

FIG. 11. The exclusive OR gate. (a) A schematic diagram of the exclusive OR function implemented using dedicated AND and OR gates. (b) An implementation of the schematic using reduced QCA logic gates. A wire crossing and an inverter are also used.

ing the ground state for each of the four possible sets of inputs that the array shown yields the truth table of an exclusive-OR function.

Figure 12 shows the schematic of our design of a single-bit full adder implemented with only inverters and majority voting logic gates. Note that no reduced gates (individual AND or OR gates) are required. The device has three inputs: the operands A_n and B_n, and the previous carry result C_{n-1}. The two outputs are the sum S_n and the carry bit C_n. Single-bit full adders like this one can be easily chained together to produce a multibit adder. Figures 13 and 14 display the ground-state charge distribution for the simulation of this device with two of the eight possible input states. These figures are the results of self-consistent Hartree calculations for the 192-cell (384 electron) system. As in previous figures, the diameter of each dot is proportional to the charge on that site. We have verified that the ground-state calculation for all eight input combinations produces output results appropriate for a full adder.

The full adder is the most complex QCA array we have simulated to date. It illustrates that it is possible to con-

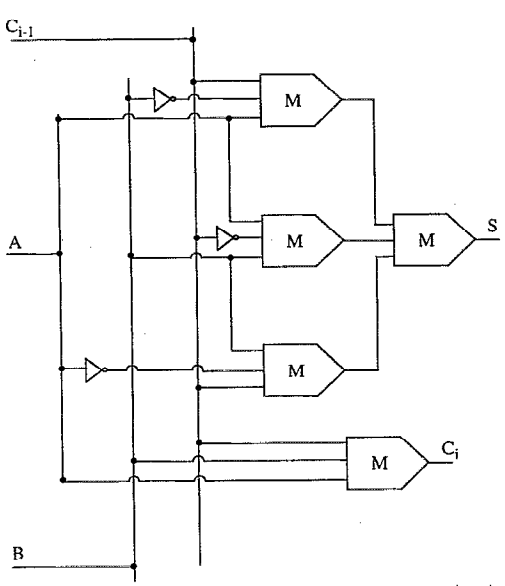

FIG. 12. The one-bit full-adder schematic diagram. This implementation uses three inverters and five majority-voting gates to perform a complicated logical calculation. Use of dedicated AND and OR gates would require a larger gate count.

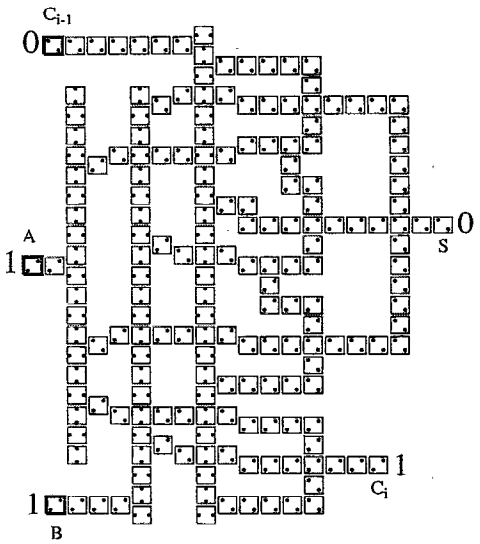

FIG. 13. The QCA full adder implementation. This figure corresponds to the schematic in Fig. 12 and uses 192 cells. The particular case shown has a zero on the carry-in line and ones on each of the addend lines. Therefore, the sum is zero and the carry-out is one. The diameter of each dot shown is proportional to the charge on the corresponding site, obtained from a self-consistent solution for the ground state charge distribution.

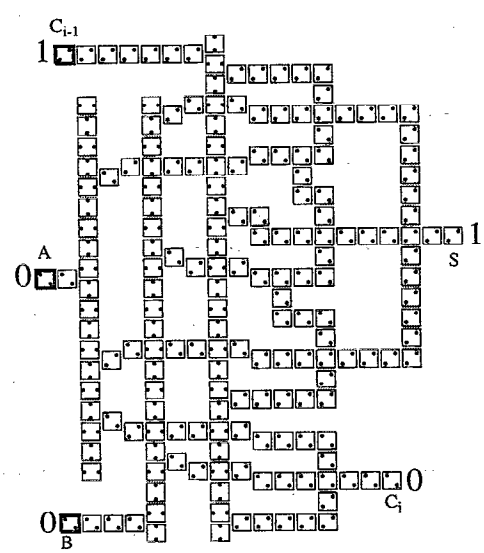

FIG. 14. The QCA full adder with different inputs. The carry-in is one and the two addends are each zero. This makes the sum one and the carry-out zero.

struct complicated arrays of cells which perform useful computing. Furthermore, a design of this size shows that the local coupling between cells lend themselves to hierarchical layout rules. The functioning of the whole array can be understood by examining the function of each part (gate, inverter, wire) independently. Although we have calculated the behavior of the system globally, by solving for the ground-state of the entire array, we can confidently predict the results by just considering each element as a separate computing component.

VII. CONCLUSIONS

Experimentally realizing cells of the type we discuss presents some challenges, but recent experiments indicate they are not insurmountable. Maintaining the double charging of each cell could be accomplished by using an insulated top gate, a conducting substrate to supply the electrons, and a thin tunnel barrier between the cells and the substrate to stabilize the charge at integer values. This method of controlling the charge state of ultrasmall structures has been demonstrated by Meuer *et al.*[12] and Ashoori *et al.*,[13] in semiconductor quantum dots. The problem of setting the polarization of a cell (writing the inputs) and sensing the polarization of a cell (reading the outputs) amounts to the problem of measuring the presence of individual electronic charges on a metal electrode. That this is feasible has been experimentally demonstrated by Field *et al.*[14]

Semiconductor fabrication of QCA devices may become possible using new nanolithographic techniques. The possibility of implementing QCA cells in small metallic islands has also been proposed.[15] Future realizations may be based on macromolecular implementations.[16] As the size of the structure is reduced, the relevant energy scales will increase leading to higher temperature operation. This *scalability* down to atomic dimensions is a key feature. The scheme does not fail as the size is reduced, rather it becomes more robust.

In conclusion, our calculations show that coupled quantum dot cells could be used to implement all three of the basic Boolean operations (AND, OR, and NOT) as well as a new primitive operation, majority voting. We have shown how linear arrays of cells can be used as binary wires, and that coplanar wire crossings are possible. By simulating an exclusive OR gate and a full adder we have demonstrated that the operation of basic QCA logical gates can be composed to form more complex device structures and that hierarchical design is possible.

ACKNOWLEDGMENTS

We gratefully acknowledge stimulating conversations with Wolfgang Porod and Gary Bernstein of the Notre Dame Nanoelectronic Group. This work was supported in part by the advanced Research Projects Agency, the Office of Naval Research, and the Air Force Office of Scientific Research. This material is based in part upon work supported under a National Science Foundation Graduate Fellowship.

[1] R. T. Bate, Bull. Am. Phys. Soc. **22**, 407 (1977); J. N. Randall, M. A. Reed, and G. A. Frazier, J. Vac. Sci. Technol. B **7**, 1398 (1989); D. K. Ferry, L. A. Akers, and E. W. Greeneich, *Ultra Large Scale Interconnect Microelectronics* (Prentice–Hall, Englewood Cliffs, NJ, 1988); J. N. Randall, A. C. Seabaugh, Y.-C. Kao, J. H. Luscombe, and B. L. Newell, J. Vac. Sci. Technol. B **9**, 2893 (1991).

[2] T. Toffoli and N. Margolus, *Cellular Automata Machines: A New Environment for Modeling* (MIT, Cambridge, MA, 1987).

[3] C. S. Lent, P. D. Tougaw, and W. Porod, Appl. Phys. Lett. **62**, 714 (1993).

[4] C. S. Lent, P. D. Tougaw, W. Porod, and G. H. Bernstein, Nanotechnology **4**, 49 (1993).

[5] C. S. Lent and P. D. Tougaw, J. Appl. Phys. **14**, 6227 (1993).

[6] P. D. Tougaw, C. S. Lent, and W. Porod, J. Appl. Phys. **74**, 3558 (1993).

[7] By contrast, these unavoidable inelastic processes are very detrimental to the operation of other quantum devices.

[8] The polarization so defined is not to be confused with a dipole moment. For the situations we consider here, the ground state of the cell has no dipole moment, though it may have a quadrupole moment. The cell polarization simply measures the degree to which the electronic charge is aligned and the direction of that alignment.

[9] For the standard cell, we take E_Q to be the Coulomb energy of two electrons separated by one-third the dot diameter D, a physically reasonable first approximation.

[10] These values of the tunneling coefficients are consistent with one-dimensional calculations for a barrier height of 150 meV. Reference 5 examines the behavior of lines of cells as all these Hamiltonian parameters are varied. The bistable behavior we examine here is not critically dependent on a particular choice of these parameters, but holds for a wide range of parameter choices.

[11] The actual neutralizing positive charge would reside on nearby metal gates and in ionized donor impurities.

[12] B. Meurer, D. Heitmann, and K. Ploog, Phys. Rev. Lett. **68**, 1371 (1992).

[13] R. C. Ashoori, H. L. Stormer, and J. S. Weiner, Physica B **184**, 378 (1993); R. C. Ashoori, H. L. Stormer, and J. S. Weiner, L. N. Pfeiffer, K. W. Baldwin, and K. W. West, Phys. Rev. Lett. **71**, 613 (1993).

[14] M. Field, C. G. Smith, M. Pepper, J. E. F. Frost, G. A. C. Jones, and D. G. Hasko, Phys. Rev. Lett. **70**, 1311 (1993).

[15] C. S. Lent and P. D. Tougaw (unpublished).

[16] For a review of the current state, see *Molecular Electronics*, edited by G. J. Ashwell (Wiley, New York, 1992).